

SMART VORTEX GENERATOR USING SHAPE MEMORY ALLOY

Tadashige Ikeda*, Shinya Masuda*, Takeshi Miyasaka**, Tetsuhiko Ueda*
*Nagoya University, **Gifu University

Keywords: *Vortex generator, Shape memory alloy, Smart structure*

Abstract

A new vortex generator (VG) concept is proposed, where VGs are effective during take-off and landing and stowed during cruise by utilizing a function of shape memory alloys (SMAs) and difference in temperature between a cruise altitude and a ground. This new VG is named Smart Vortex Generator (SVG). Numerical simulation using a simplified mathematical model of SVG indicates that temperature of SVG can follow an ambient temperature change during descending/ascending and SVG can change its shape between a stowed position and a vortex-generating position. Moreover, a conceptual demonstration model of SVG is made of SMA ribbons and ribbon springs. This demonstration model verifies that SVG can be practically transformed between the two positions by cooling and heating.

1 Introduction

Vortex generators (VGs) are devices to delay or prevent flow separation by generating vortexes and mixing flow. They are usually solid vanes and fixed on surfaces of vehicles, turbo-machines, etc. For some airplanes' wings VGs are necessitated during take-off and landing, when the wings have a high angle of attack and a large camber. However, they have an adverse effect during cruise because of their useless drag. It is cumbersome if we think of time for cruise much longer than for take-off and landing. Hence some types of controllable VGs have been proposed [1, 2].

Barrett and Farokhi [1] proposed a controllable ramp type VG system. This VG system consisted of a steel ramp type VG with a shape memory alloy (SMA) wire actuator and a steel wire spring, a shear-flow sensor, and an optimum controller. The height of VGs was controlled by applying electric current to the SMA actuator as a function of strength of shear flow. A lift-drag performance of a wing with this VG system became better compared to a clean wing or a wing with fully extended VGs.

Campbell [2] proposed a fin type controllable VG, which was composed of a fin made of SMA, a leaf spring, a base, and a heating element. The SMA fin remembered a straight shape and was hooked to the curved leaf spring to be in a deflected position at a low temperature. When the fin was heated by the heating element, it moved from the deflected position to an undeflected position, and reduced the drag. When the current to the heating element was turned off, it returned to the deflected position by the spring.

As shown above, the conventional controllable VGs need energy to change their positions. The energy for controlling VG may become larger than energy saved. Furthermore, sensors, controllers, and wiring are needed. Accordingly, it is not easy to install such VG systems into existing aircrafts.

Therefore, we propose a new VG concept where VGs change their shape autonomously so as to be in a stowed position during cruise and in a vortex-generating position during take-off and landing by utilizing a function of SMA and difference in temperature between a cruise altitude and a ground. This new VG is named Smart Vortex Generator (SVG). In this paper, in

particular, we numerically examine whether temperature of a SMA element in SVG can follow an ambient temperature change during descending and whether enough strain of the SMA element can be obtained to change the SVG shape between the two positions. Moreover, a conceptual demonstration model of SVG is made of SMA ribbons and we examine whether it can change its shape practically by cooling and heating.

2 Structure of SVG

SMA has unique properties such as shape memory effect and superelasticity, as shown in Fig. 1. They are caused by a phase transformation between an austenite phase and a martensite phase. The austenite phase of NiTi SMA has a cubic crystal structure and it is stable at a higher temperature and a lower stress, while the martensite phase has a monoclinic crystal structure and it is stable at a lower temperature and a higher stress. The recoverable strain of the shape memory effect and the superelasticity is 5 to 10 %. Moreover, a yielding stress, that is a transformation stress, decreases with a decrease in temperature. With respect to the temperature, an ambient temperature at a cruise altitude of a jet airliner (approximately 11 km) is approximately 70 K lower than at a ground.

From the above facts we considered that a shape of VG can be controlled without energy input, by making VG of SMA and using the temperature difference between the cruise altitude and the ground as a control input. Benefits of this VG are no energy input, easy installation, maintenance free, etc.

An example of SVG structure is shown in Fig. 2. This SVG consists of a curved SMA plate and a curved blade spring only. At a natural state on the ground, the SMA plate is in the austenite phase remembering a curved shape and the blade spring has curves in the opposite direction. The spring is hooked to the SMA plate to form SVG. At a temperature near the ground, SMA is stiff enough not to lie down by the spring. On ascending, as the temperature

decreases, the yielding stress of the SMA plate decreases so that the SMA plate is lying down gradually. During cruise when the temperature is low and the stiffness of the SMA plate is also low enough for it to lie down completely to the stowed position. On descending, SVG sits up again.

This SVG is a kind of smart structures because it can autonomously change its shape appropriately according to a change in ambient temperature, that is a change in altitude. Energy input is not necessary for this SVG to be activated. Moreover, its structure is very simple.

3 Feasibility Study

We examined if SVG could work or not theoretically using a simplified mathematical model shown in Fig 3. A SMA plate of SVG was assumed to obey the beam theory. The force of the blade spring was approximated by a bending moment proportional to an angle of the SMA plate, θ . Considering a line element of the SMA plate at a certain position from the neutral axis, the element was approximated by a SMA wire connected to a spring. This system was considered as a simplified SVG model.

3.1 Constitutive Model of SMA

To examine behavior of the SMA wire as a representative of the SVG, Ikeda et al.'s one-dimensional phase transformation model was adopted as a constitutive model of SMA, which is simple and reasonably accurate [3-5]. This constitutive model is briefly reviewed below.

The concept of the one-dimensional phase transformation model is illustrated in Fig. 4. Here we consider a SMA wire specimen. In this model, virtual grains are sorted in order of energy required for transformation due to internal friction between phases and grains (RTE: the required transformation energy) so that RTE takes the minimum value at the bottom and the maximum value at the top. The order of these grains is assumed to be unchanged irrespective of phases before and after the transformation. Accordingly, each phase transformation takes place from a lower

part to an upper part of the specimen. The specimen is assumed to consist of two phases; the austenite phase (phase A) and the martensite phase (phase M). First, a whole specimen is assumed to be in phase A (Fig. 4 (a)). When a tensile force is loaded to the specimen and a stress value increases beyond a certain critical value, a transformation from phase A to phase M takes place from the bottom, at which RTE takes the minimum value (Fig. 4 (b)). Then, when the force is unloaded, a transformation from phase M to phase A takes place from the bottom (Fig. 4 (c)). Finally, when the specimen is heated keeping the force, a transformation from phase M to phase A takes place from the location with the minimum energy value in phase M (Fig. 4 (d)).

Since the phase transformations take place one-dimensionally as shown in Fig. 4, this model is named the one-dimensional phase transformation model. A sum of ranges for the same phase corresponds to a volume fraction of the phase, when a distance from the bottom is normalized with the total length of the specimen. Hence, the ordinate is named the volume fraction coordinate (VFC).

According to the above assumption, we formulate a transformation criterion. The transformation criterion from phase α to phase β is given by

$$\begin{aligned} & \frac{1}{2} \sigma^2 \left(\frac{1}{E_\beta} - \frac{1}{E_\alpha} \right) + \sigma (\varepsilon_\beta - \varepsilon_\alpha) \\ & + (s_\beta - s_\alpha) (T - T_{\alpha \leftrightarrow \beta}) \\ & = \Psi_{\alpha \rightarrow \beta} (z_{\alpha 1}), \quad (1) \end{aligned}$$

where σ , E_α , ε_α , s_α , T , and $T_{\alpha \leftrightarrow \beta}$ denote the stress of SMA, the Young's modulus of phase α , the intrinsic strain, the entropy, the material temperature, and the ideal transformation temperature between phase α and phase β for free stress and no dissipation due to the internal friction. The left-hand side of the equation is the thermodynamic driving energy for the phase transformation. The right-hand side, $\Psi_{\alpha \rightarrow \beta}$, is RTE from phase α to phase β , where $z_{\alpha 1}$ denotes the minimum VFC of phase α shown in Fig. 4.

When the driving energy becomes equal to RTE, the phase transformation is assumed to take place.

Strain is assumed to consist of elastic, transformation, and thermal parts, and is given by

$$\varepsilon = \sum_{\alpha} \left(\frac{\sigma}{E_\alpha} + \varepsilon_\alpha \right) z_\alpha + \alpha_T (T - T_i), \quad (2)$$

where z_α , α_T , and T_i are the volume fraction of phase α , the thermal expansion coefficient, and the initial temperature.

The energy balance equation is given by

$$\begin{aligned} & C\dot{T} + \sum_{\alpha \rightarrow \beta} (s_\beta - s_\alpha) T \dot{z}_{\alpha \rightarrow \beta} + \alpha_T T \dot{\sigma} \\ & = -h \frac{A}{V} (T - T_s) + \sum_{\alpha \rightarrow \beta} \Psi_{\alpha \rightarrow \beta} \dot{z}_{\alpha \rightarrow \beta}. \quad (3) \end{aligned}$$

The dot over variables is used to describe the time derivative. C , h , and A/V are the specific heat capacity at constant stress, the convection heat transfer coefficient, and the ratio of the exposed area to the volume of the specimen, respectively. The second term of the left hand side represents the latent heat, the third term the thermoelastic effect, the first term of the right hand side the heat exchange between SMA and the surroundings, and the last term the heat generated due to the internal friction.

3.2 Numerical Results

First, temperature change of the SMA element during descending was examined. In this simulation, an airplane was assumed to descend from a cruise state with an altitude of 11 km, an ambient temperature of -56.4 °C, and an airspeed of 900 km/h to a landing state with an altitude of 0 km, a temperature of 15 °C, and an airspeed of 300 km/h. Two cases were calculated for different descending time; 1800 s and 900 s.

Assuming the latent heat, the thermoelastic effect, and the generated heat to be negligible small compared to the heat exchange in Eq. (3), and using a wire with a diameter of d as a

representative of SVG, the energy balance equation is reduced to

$$C\dot{T} = -h\frac{4}{d}(T - T_s). \quad (4)$$

h is determined by [6]

$$h = 0.193\frac{k}{d}\left(\frac{U_\infty d}{\nu}\right)^{0.618}\frac{1}{\text{Pr}^{\frac{1}{3}}}, \quad (5)$$

where k , U_∞ , ν , and Pr denote the heat transfer coefficient of air, the airspeed, the kinematic viscosity, and Prandtl number. Based on the data of the standard atmosphere [7], T_s [$^{\circ}\text{C}$], k [$\text{W}/(\text{m}\cdot\text{K})$], ν [m^2/s], Pr are given by the functions of the altitude, Z [m],

$$\begin{aligned} T_s &= -0.00649Z + 15.0, \\ \nu &= 1.22 \times 10^{-13} Z^2 + 8.25 \times 10^{-10} Z + 1.49 \times 10^{-5}, \\ k &= -5.29 \times 10^{-7} Z + 0.0254, \\ \text{Pr} &= 2.04 \times 10^{-6} Z + 0.710. \end{aligned} \quad (6)$$

The temperature change of SMA wire with $d = 0.75$ mm and $C = 3.0$ MJ/($\text{m}^3\cdot\text{K}$) against the ambient temperature change during the descending is shown in Fig. 5. It can be seen from this figure that the temperature of SMA smoothly follows the ambient temperature for both the cases. This is because the airspeed is high enough for good heat transfer between SMA and the surroundings.

Next, substituting $T = T_s$ into Eq. (1) according to the above result, neglecting the thermal expansion term, and applying the recovery stress of the spring, we examined the motion of SVG against the ambient temperature change. The stress-strain relationship of the spring was approximated by

$$\sigma = -E_s(\varepsilon - \varepsilon_i), \quad (7)$$

where E_s is the effective Young's modulus of the spring and ε_i is the gap between the SMA line element and the spring at a natural state. RTE was approximated by [3-5]

$$\Psi_{\alpha \rightarrow \beta} = \Psi_c \left\{ 1 - a_1^{-z_{\alpha \rightarrow \beta}} + a_2^{-(1-z_{\alpha \rightarrow \beta})} \right\}. \quad (8)$$

The material constants used in the simulation are listed in Table 1. Stress-strain relationships of the SMA line element only at temperatures of 15, -10 , and -35 $^{\circ}\text{C}$ are shown in Fig. 1, where the initial phase was assumed to be the austenite.

Fig. 6 shows the strain of the SMA line element of SVG against the ambient temperature change. The strain of the element is compared between $E_s = 1$ GPa and 10 GPa. For $E_s = 1$ GPa, the strain is less than 0.1 % around the ground, gets large around -35 $^{\circ}\text{C}$, and finally becomes 3 % at the cruise. When the airplane returns to the ground, the strain recovers. The recoverable strain is about 3 %. The 3 % of strain is enough for SVG to lie down at the cruise and sit up around the ground. For $E_s = 10$ GPa, the initial strain is larger and the temperature range for the transformation is also larger than for $E_s = 1$ GPa. The former makes the recoverable strain smaller and the latter makes the response of the transformation against the ambient temperature worse.

4 Conceptual Demonstration Model

To verify that SVG can work, a conceptual demonstration model of SVG was made. It was composed of SMA ribbons welded and ribbon springs as shown in Fig. 7. The austenite transformation finish temperature of the SMA ribbons was controlled at approximately 50 $^{\circ}\text{C}$ so as to observe a motion using a hot air blower. It is noted that SVG to be installed into real aircrafts will be made of a SMA plate and its austenite transformation finish temperature will be controlled at approximately -40 $^{\circ}\text{C}$.

By cooling the SVG model with a cold gas spray to simulate ascending, the SVG was lying down, and by heating with a hot air blower to simulate descending, the SVG model was sitting up. This shows that SVG can be practically transformed by changing the ambient temperature only.

5 Summary

A new smart vortex generator concept was proposed, which is effective during take-off and landing only and stowed during cruise by utilizing a function of shape memory alloys. It was shown with a simplified mathematical model and a conceptual demonstration model that this smart vortex generator could be transformed between a stowed position and a vortex-generating position by changing an ambient temperature only.

Acknowledgements

A part of this research was supported by C-ASTEC (Chubu Aerospace Technology Center).

References

- [1] Barrett R and Farokhi S. Subsonic aerodynamics and performance of a smart vortex generator system. *J. Aircraft*, Vol. 33, No. 2, pp 393-398, 1996.
- [2] Campbell M. Controllable vortex generator. *United States Patent*, No. US 6,427,948 B1, 2002.
- [3] Ikeda T et al. Constitutive model of shape memory alloys for unidirectional loading considering inner hysteresis loops. *Smart Materials and Structures*, Vol. 13, pp 916-925, 2004.
- [4] Ikeda T. Modeling of ferroelastic behavior of shape memory alloys. *Proc. SPIE*, Vol. 5757, pp 344-352, 2005.
- [5] Ikeda T. Application of one-dimensional phase transformation model to tensile-torsional pseudoelastic behavior of shape memory alloy tubes. *Proc. SPIE*, Vol. 6166, pp 61660z-1-61660z -8, 2006.
- [6] Holman J P. *Heat transfer*, 5th edition, McGraw-Hill, 1981.
- [7] JSASS. *Aerospace engineering handbook*, Maruzen, 2005.

Table 1 Material constants of the SMA line element and the spring

Constant	Value
E_A	40 GPa
E_M	20 GPa
E_S	10 GPa / 1.0 GPa
ϵ_A	0.0
ϵ_M	0.030
ϵ_i	0.031
$s_{M \rightarrow SA}$	-0.25 MJ/(m ³ K)
$T_{A \leftrightarrow M}$	-35 °C
Ψ_c	1.0 MJ/m ³
a_1	1.0×10^6
a_2	1.0×10^6

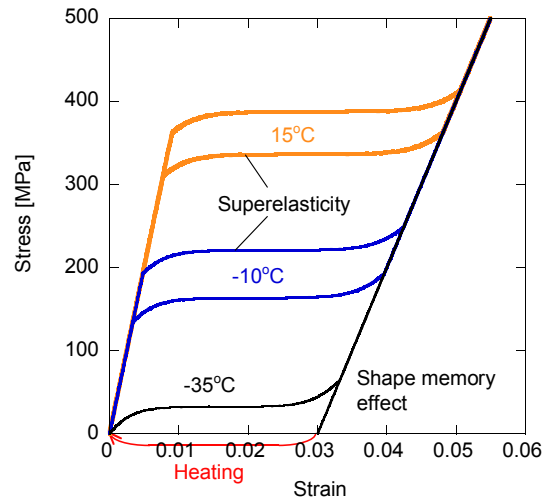


Fig. 1 Stress-strain relationship of SMA

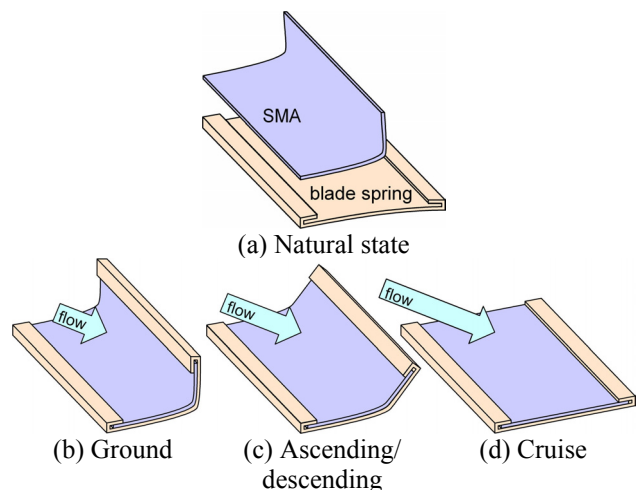


Fig. 2 Example structure of SVG

